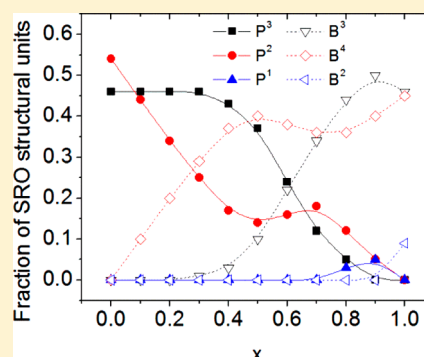


Structural Studies of Mixed Glass Former $0.35\text{Na}_2\text{O} + 0.65[x\text{B}_2\text{O}_3 + (1 - x)\text{P}_2\text{O}_5]$ Glasses by Raman and ^{11}B and ^{31}P Magic Angle Spinning Nuclear Magnetic Resonance Spectroscopies

Randilynn Christensen,[†] Garrett Olson, and Steve W. Martin*

Department of Materials Science and Engineering, Iowa State University, Ames, Iowa 50011, United States

ABSTRACT: The mixed glass former (MGF) effect (MGFE) is defined as a nonlinear and nonadditive change in the ionic conductivity with changing glass former composition at constant modifier composition. In this study, sodium borophosphate $0.35\text{Na}_2\text{O} + 0.65[x\text{B}_2\text{O}_3 + (1 - x)\text{P}_2\text{O}_5]$, $0 \leq x \leq 1$, glasses which have been shown to exhibit a positive MGFE have been prepared and examined using Raman and ^{11}B and ^{31}P magic angle spinning nuclear magnetic resonance (MAS NMR) spectroscopies. Through examination of the short-range order (SRO) structures found in the ternary glasses, it was determined that the minority glass former, B for $0.1 \leq x \leq 0.7$ and P for $0.7 \leq x \leq 0.9$, is “overmodified” and contains more Na^+ ions than would be expected from simple linear mixing of the binary sodium borate, $x = 1$, and sodium phosphate, $x = 0$, glasses, respectively. Changes in the intermediate range order (IRO) structures were suggested by changes in the NMR spectral chemical shifts and Raman spectra wavenumber shifts over the full composition range x in the Raman and MAS NMR spectra. The changes observed in the chemical shifts of ^{31}P MAS NMR spectra with x are found to be too large to be caused solely by changing sodium modification of the phosphate SRO structural groups, and this indicates that internetwork bonding between phosphorus and boron through bridging oxygens (BOs), $\text{P}-\text{O}-\text{B}$, must be a major contributor to the IRO structure of these glasses. While not fully developed, a first-order thermodynamic analysis based upon the Gibbs free energies of formation of the various SRO structural units in this system has been developed and can be used to account for the preferential formation of tetrahedral boron groups, B^4 , by the reaction of B^3 with P^2 groups to form B^4 and P^3 groups, respectively, where the superscript denotes the number of BOs on these units, in these glasses. This preference for B^4 units appears to be a predominate cause of the changing modifier to glass former ratio with composition x in these ternary MGF glasses and appears to be associated with the large negative value of the Gibbs free energy of formation of this group.



1. INTRODUCTION

1.1. Background. Energy storage is a growing concern in an ever increasingly battery driven society. Batteries power everything from cell phones to computers to medical devices to automobiles. The development of safer, smaller, and more energy dense batteries is in demand. Ion conducting glasses are an important type of solid electrolyte that may be used to answer this need. A currently unexplained change in the ionic conductivity in glasses known as the mixed glass former effect (MGFE) has been seen in many mixed glass former (MGF) glasses^{1–8} such as $\text{Li}_2\text{S} + \text{GeS}_2 + \text{GeO}_2$ glasses⁹ and $\text{Li}_2\text{S} + \text{SiS}_2 + \text{GeS}_2$ glasses.³ This change in the ionic conductivity is nonlinear and nonadditive and can be observed as either negative or positive with changing glass former fraction at constant modifier composition between the two binary glass forming systems. A positive MGFE with a maximum deviation from linearity at $x = 0.4$ has been observed in the $0.35\text{Na}_2\text{O} + 0.65[x\text{B}_2\text{O}_3 + (1 - x)\text{P}_2\text{O}_5]$ glasses under study in this work and is shown in Figure 1.¹⁰ While this phenomena has not been fully explained,^{2,3,7,11} increases in the ionic conductivity of up to 2 orders of magnitude have been observed in other MGF glasses reported in the literature.^{1,2} Understanding the cause of

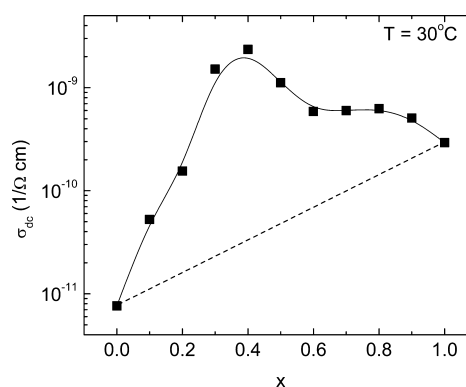


Figure 1. Composition dependence of the ionic conductivity of $0.35\text{Na}_2\text{O} + 0.65[x\text{B}_2\text{O}_3 + (1 - x)\text{P}_2\text{O}_5]$ glasses at 30°C .

the MGFE is crucial to the effort of engineering solid electrolyte glasses with even higher ionic conductivities. It is

Received: August 27, 2012

Revised: January 2, 2013

Published: January 2, 2013

our hypothesis that structural changes at the short-range order (SRO) level, caused by the mixing of the two glass former networks, are the underlying causes of the MGFE. These changes at the SRO level must necessarily effect changes at the intermediate range order (IRO) level as well. In order to confirm this hypothesis, the links between the physical properties, structure, and composition of MGF glasses are being explored.

To better understand the effect of composition on the physical properties and structure of these ternary MGF glasses, all components of the glasses in the present study were carefully chosen. Oxygen was selected as the anion with Na, P, and B as the cations. Boron and phosphorus were chosen because of their nuclear magnetic resonance (NMR) spectroscopy accessible isotopes, ^{11}B and ^{31}P . Oxygen was chosen as the anion because of the strong glass forming ability of B_2O_3 and P_2O_5 . Sodium was chosen as the glass modifier and ionic charge carrier because its radioactive isotope ^{22}Na is useful for tracer diffusion measurements and the isotope ^{23}Na is useful in NMR studies. In addition, B_2O_3 ^{12–14} and P_2O_5 ¹⁵ glasses, their binary glassy counterparts, $\text{Na}_2\text{O} + \text{B}_2\text{O}_3$ ^{14,16} and $\text{Na}_2\text{O} + \text{P}_2\text{O}_5$,^{17–20} and some ternary alkali borophosphate glasses^{8,21–24} have been well studied and reported in the literature. The literature reports on the structures of the binary glasses have been used in this study to verify the $x = 0$ and $x = 1$ experimental data in this study and to provide starting points for the analysis of the structures of the ternary sodium borophosphate glasses with $0.1 \leq x \leq 0.9$.

1.2. Glass Structure Notations. The short-range glass structures will be referred to as P^n_{mK} and B^n_{mK} where P and B are the glass formers connected to n number of bridging oxygens (BOs), m number of the BOs bonding to glass former K, and $n - m$ BOs bonded to the glass former. For example, P^n_{mB} indicates a phosphorus atom with n number of BOs that bond to m number of boron atoms and $(n - m)$ number of phosphorus atoms. If no mK is denoted, then it is unknown what glass former is being bonded to by the BO. The SRO structures present in the binary borate and phosphate glasses are shown in Figures 2 and 3, respectively.

1.3. Glass Modifier to Glass Former Ratio Notation. When discussing the number of sodium ions ionically bonded to a glass former structural unit, the ratio Na:B or Na:P will be used. Na represents the mole fraction of Na ionically bonded to the glass former, B or P. B and P represent the total mole fraction of boron or phosphorus, respectively, in the glass. If

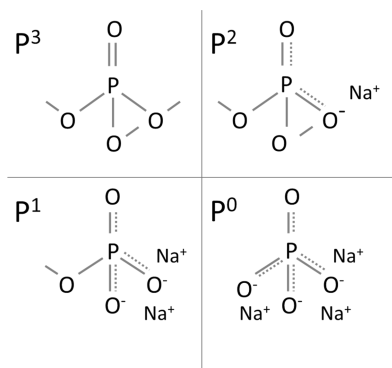


Figure 2. Binary sodium phosphate glass SRO structures, $y\text{Na}_2\text{O} + (1 - y)\text{P}_2\text{O}_5$. P^3 is present from $0 \leq y < 0.5$, P^2 is present from $0 < y < 0.65$, P^1 is present from $0.5 < y$, and P^0 is present from $0.65 < y$.

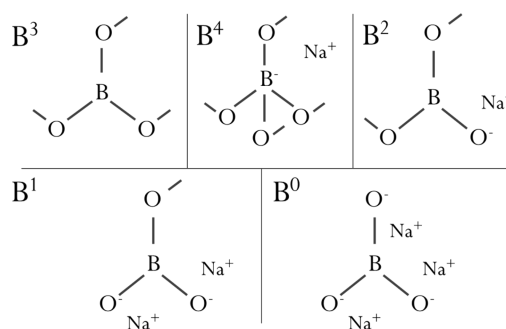


Figure 3. Binary sodium borate glass SRO structures, $y\text{Na}_2\text{O} + (1 - y)\text{B}_2\text{O}_3$. B^3 is present from $0 \leq y < 0.25$, B^4 is present from $0 < y$, B^2 is present from $0.3 < y < 0.7$, B^1 is present from $0.45 < y$, and B^0 is present from $0.55 < y$.

this ratio is equal to that of the binary glasses and remained constant across the full compositional range of the ternary glasses, x , then at each composition the ratios Na:B and Na:P would both be equal to 0.35:0.65. However, we will show that the sharing of Na between the phosphorus and boron SRO structures is non-proportional across the ternary compositions of these glasses and that, in these glasses, this ratio becomes more or less than that in the binary glasses, 0.35:0.65, as one of the glass formers bonds to more or less sodium through nonbridging oxygens (NBOs) than in the corresponding binary end member glasses. For example, a Na:B ratio of 0.7:1.17, which reduces to 0.35:0.585, in a $0.35\text{Na}_2\text{O} + 0.65[x\text{B}_2\text{O}_3 + (1 - x)\text{P}_2\text{O}_5]$ glass at $x = 0.9$, means that 0.7 mol or 100% of the Na in the glass is ionically bonded to 1.17 mol of boron in various boron SRO structural units. In this case, the ratio of Na:P must be 0:0.065, where there are 0 mol of Na ionically bonded to the 0.13 mol of phosphorus present in the glass. However, even when nonproportional sharing of the Na occurs between B and P SRO structural units, the ratio of modifier to total glass former Na:[B+P] is always equal to 0.35:0.65.

2. EXPERIMENTAL METHODS

2.1. Sample Preparation. The starting materials used to prepare the glasses were sodium carbonate (Na_2CO_3 , 99.5% Fisher Scientific), ammonium hydrogen phosphate dibasic ($(\text{NH}_4)_2\text{HPO}_4$, 98.8% Fisher Scientific), and boric acid (H_3BO_3 , 99.5% Fisher Scientific). After weighing and mixing the appropriate amounts, the starting materials were calcined in platinum crucibles between 900 and 1100 °C for 0.5–1 h in an electric furnace in a fume hood. After the melt was bubble free, the crucible was removed from the furnace and allowed to cool to room temperature. Once cool, the sample was weighed to determine the weight lost from NH_3 , H_2O , and CO_2 . Samples were found to be within ± 1.5 wt % of their target weight. These slightly hygroscopic samples were then transferred to a high quality nitrogen atmosphere glovebox (< 5 ppm O_2 and H_2O) and remelted in an electric furnace at 1000–1100 °C for 10 min. To create bulk samples of these glasses, the melt was quenched in preheated brass molds at temperatures 40 °C below the glass transition temperature (T_g). Bulk samples were round discs approximately 20 mm in diameter and 2 mm thick. The bulk samples were annealed 40 °C below the T_g for 0.5 h and then cooled to room temperature at a rate of 2 °C/min. Due to their hygroscopic character, all samples were stored in the N_2 atmosphere glovebox. All of the glasses were checked for crystallization with X-ray diffraction (XRD) and found to be X-

ray amorphous. Sodium, oxygen, and phosphorus concentrations were checked by energy dispersive spectroscopy (EDS) and found to be within ± 4 at. % of their batched compositions. Infrared spectroscopy was used to ensure that all of the glasses did not contain residual NH_3 , CO_2 , and H_2O .

2.2. Raman Spectroscopy. Raman spectra were collected using a Renishaw InVia Raman Spectrometer Microscope. The instrument was calibrated using an internal silicon reference with a peak at 520.5 cm^{-1} , and the peaks were reproducible to within $\pm 1\text{ cm}^{-1}$. An argon laser at 488 nm with 20 mW of power was used for excitation, and spectra were acquired using two accumulations of 10 s at 100% power using a $20\times$ working objective lens on a bulk glass sample. Spectra from various spots across the surface of the glass were taken and were found to be identical, suggesting that the glasses are homogeneous.

2.3. Magic Angle Spinning Nuclear Magnetic Resonance (MAS NMR) Spectroscopy. Single pulse ^{31}P and ^{11}B MAS NMR spectra were obtained using a Bruker AV-600 Spectrometer using a 4 mm zirconia probe spinning at 12 and 10 kHz , respectively. ^{31}P MAS NMR spectra were measured at 242.95 MHz with a 90° pulse of $2\text{ }\mu\text{s}$, a delay of 300 s , and 16 scans. ^{11}B MAS NMR spectra were recorded at 192.55 MHz using a 25° tipping angle pulse of $1\text{ }\mu\text{s}$, a delay of 3 s , and 40 scans. The tipping angle of the boron spectra was determined by finding the pulse length where the resulting area of the spectral peaks arising from trigonal and tetrahedral borons were equal in a sample of borax ($\text{Na}_2\text{B}_4\text{O}_7 \cdot 10\text{H}_2\text{O}$, Fisher Scientific, 99.5%). Borax has been shown by X-ray crystallography to contain equal amounts of trigonally and tetrahedrally coordinated boron atoms.²⁵ Chemical shifts were reported relative to 85% phosphoric acid, H_3PO_4 , for ^{31}P and $\text{BF}_3\text{--Et}_2\text{O}$ solution for ^{11}B . Examples of the ^{31}P and ^{11}B MAS NMR spectra for selected ternary glasses are shown in Figures 4 and 5, respectively.

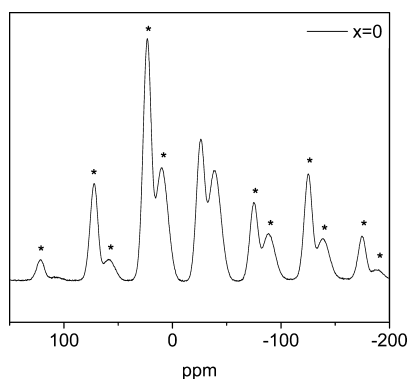


Figure 4. Example of ^{31}P MAS NMR spectra at $x = 0$, where the asterisks indicate spinning sidebands.

3. RESULTS

3.1. Short Range Order Structures from Raman Spectroscopy. The Raman spectra of $0.35\text{Na}_2\text{O} + 0.65[x\text{B}_2\text{O}_3 + (1-x)\text{P}_2\text{O}_5]$ glasses are shown in Figure 6 and are comparable to spectra found in the literature for similar glasses.^{18,26–30} Due to the stronger Raman scattering cross section of the phosphate SRO structural units than the borate SRO structural units, the Raman spectra of sodium borophosphate glasses show Raman bands that are far more intense for the modes arising from the phosphate structural

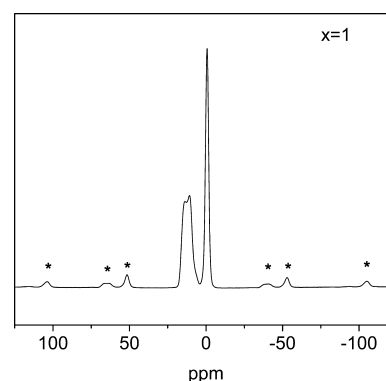


Figure 5. Example of ^{11}B MAS NMR spectra at $x = 1$, where the asterisks indicate spinning sidebands.

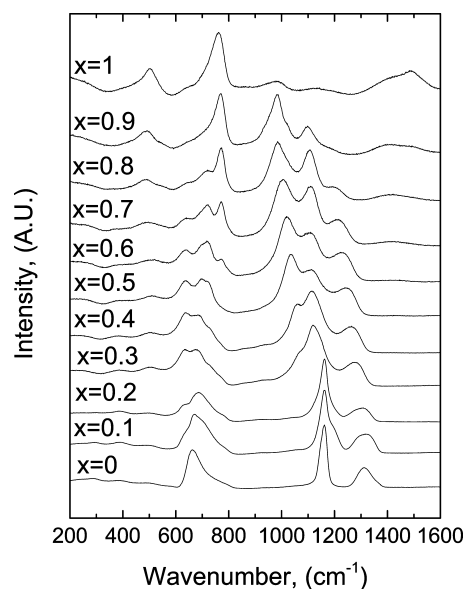


Figure 6. The compositional dependence of the Raman spectra of $0.35\text{Na}_2\text{O} + 0.65[x\text{B}_2\text{O}_3 + (1-x)\text{P}_2\text{O}_5]$ glasses.

units than the modes arising from the borate structural units. However, as is the common practice in Raman spectroscopy, we have scaled each spectrum to the same intensity for the strongest peak. The result of such scaling produces Raman spectra that are more easily interpreted but masks the underlying sensitivity difference between B and P Raman peaks.

3.1.1. Raman Spectra of the $x = 0$ Glass. The Raman spectrum of the binary $0.35\text{Na}_2\text{O} + 0.65\text{P}_2\text{O}_5$ glass shows three main peaks at 665 , 1164 , and 1315 cm^{-1} . The broad peak at 665 cm^{-1} arises from the symmetric stretching of the BO in the P--O--P linkage.¹⁸ The peak at 1164 cm^{-1} is assigned to the symmetric stretch of the two NBO, present in a P_2^2 unit, the $(\text{PO}_2)_{\text{sym}}$ mode, and the 1315 cm^{-1} peak is assigned to the phosphorus double bonded oxygen symmetric stretching mode found only in P_3^3 units, the $(\text{P=O})_{\text{sym}}$ mode.^{18,28}

3.1.2. Raman Spectra of the $0.1 \leq x \leq 0.2$ Glasses. When boron is added to the binary sodium phosphate glass at $x = 0.1$ and 0.2 , the spectra show that several changes must be occurring in the glass structure. In addition to the previously discussed $(\text{PO}_2)_{\text{sym}}$ stretch at 1164 cm^{-1} , the P_2^2 unit now also shows an asymmetric stretching mode at 1280 cm^{-1} .²⁸ The peaks at 1190 and 1330 cm^{-1} are “strained” variants of the symmetric and asymmetric P_2^2 stretches, respectively.²⁸ These

variations each have a specific structure that differs from the normal P^2 modes. In their studies of binary lithium phosphate glasses, Hudgens et al.²⁸ associated these strained modes with rings composed of P^3 and P^2 units or a cross-linking P^3 unit between metaphosphate, P^2 , chains. The ^{11}B NMR spectra, to be discussed below, will show that at $x = 0.1$ the only boron unit present is the B^4 unit even though the literature on the binary $0.35\text{Na}_2\text{O} + 0.35\text{B}_2\text{O}_3$ glass suggests that both B^2 and B^3 units should also be present.³¹ At this $x = 0.1$ composition, it is assumed that the B^4 unit bridges primarily to phosphorus given the small numbers of boron atoms in the glass at $x = 0.1$, $\text{B}:\text{P} = 1:9$. Two possible structural changes could be taking place to explain these results. First, the added boron could remove sodium from the P^2 units to modify the B^3 unit to form the observed B^4 units, causing the formation of cross-linked metaphosphate chains or rings of P^3 and P^2 units in a $P^2 + B^3 \rightarrow P^3 + B^4$ reaction. The second possibility is that a B^4 unit is formed as a part of a phosphate chain or ring, forming $P^n\text{--O--B}^4\text{--O--P}^n$ bonds, where $n = 3$ or 2 .

In these predominately phosphorus rich glasses, the peak at 665 cm^{-1} develops shoulders at 630 , 690 , and 775 cm^{-1} with added B_2O_3 . In binary sodium borate glasses, peaks in this region originate from vibrations of the metaborate, $0.5\text{Na}_2\text{O} + 0.5\text{B}_2\text{O}_3$, superstructural unit. However, a metaborate superstructural unit is composed of three trigonal B^2 boron units that form a six-membered ring and we will show below that only B^4 units are observed in the ^{11}B MAS NMR spectra until $x = 0.3$, where only a barely detectable 2% of the boron are in trigonal B^3 coordination. Therefore, the peaks at 630 , 690 , and 775 cm^{-1} cannot arise from metaborate units. Hudgens et al. suggested that a peak at 775 cm^{-1} corresponds to the asymmetric stretch of the BO linking two phosphorus in the $(\text{POP})_{\text{asym}}$ stretch mode in $P^2_{\text{mP}^2}$, $P^2_{\text{mP}^3}$, and $P^3_{\text{mP}^3}$ units in binary lithium phosphate glasses.²⁸ Therefore, we attribute the 630 and 690 cm^{-1} shoulder peaks to the POB stretches in $P^2_{\text{mB}^4}$ and $P^3_{\text{mB}^4}$ units and the shoulder at 775 cm^{-1} to the asymmetric stretches of POP structures.

3.1.3. Raman Spectra of the $0.3 \leq x \leq 0.5$ Glasses. For the $x = 0.3$ glass, the mode arising from P^2_{P} units and assigned to the peak at 1164 cm^{-1} is joined by a shoulder at 1124 cm^{-1} , indicating a possible change in the next nearest neighbor bonding to this unit, such as the formation of P^2_{IB} units. At an even lower frequency, the peak at 1059 cm^{-1} is assigned to the symmetric stretch of the P^2_{IB} unit. As the boron content increases, the peaks at 1124 and 1315 cm^{-1} shift to lower frequencies, indicating the progressive replacement of P^2_{P} by P^2_{IB} units and P^3_{P} by P^3_{IB} units, respectively.

A new peak at 720 cm^{-1} appears in the Raman spectrum of the $x = 0.3$ glass. We assign this peak to the ring breathing vibrations of six-membered rings containing a trigonal boron and two B^4 units. This assignment is supported by the presence of both trigonal and tetrahedral boron peaks in the ^{11}B NMR spectrum of this glass composition; see below. The weak peak at 505 cm^{-1} is attributed to diborate groups or rings with one or two B^4 units.^{26,32} This is the first indication of trigonal boron units in the structure of these glasses, as suggested by the Raman spectra.^{27,32,33}

3.1.4. Raman Spectra of the $0.6 \leq x \leq 0.9$ Glasses. In the Raman spectrum of the $x = 0.6$ glass, the peak at 720 cm^{-1} is joined by a peak at 770 cm^{-1} and we assign the latter to the ring breathing vibrations of six-membered rings containing two trigonal boron units and one B^4 unit. The increasing intensity of the peak at 770 cm^{-1} and the decreasing intensity of the peak

at 720 cm^{-1} suggest that the number of trigonal borons is increasing faster than the number of tetrahedral borons. For the glass at $x = 0.8$, a new shoulder appears at 990 cm^{-1} . At the same composition, the ^{31}P MAS NMR spectra, shown below, suggest the presence of P^1 units, although P^1 units are not present in binary 0.35 sodium phosphate glasses. However, in the Raman spectrum of the binary $0.65\text{Na}_2\text{O} + 0.35\text{P}_2\text{O}_5$ glass, the P^1 mode is at $\sim 1025\text{ cm}^{-1}$. Due to the predominance of boron in the $x = 0.8$ ternary glass composition, $\text{B}:\text{P} = 4:1$, it is likely that the P^1 unit has its one BO bonded to a boron atom, which would cause a shift in this peak position to lower wavenumbers.¹⁸ Therefore, we can assign this new peak at 990 cm^{-1} to a vibrational mode of the P^1_{IB} unit.

The vibrational modes of the P^1 , P^2 , and P^3 units are present in the glasses up until $x = 0.9$. However, the changing intensity of these peaks suggests that, at $x = 0.8$, P^3 units are transformed to P^1 units, where the chemical reaction $2B^4 + P^3 \rightarrow 2B^3 + P^1$ would be consistent with this compositional change of these SRO structural units. Although both the P^1 and P^2 peaks overlap with peaks arising from the boron diborate group, the weak intensity of the diborate peak at $x = 1$ suggests that the diborate contribution to the peak intensity in the ternary glasses is small.

3.1.5. Raman Spectra of the $x = 1$ Glass. The Raman spectrum of the binary sodium borate glass at $x = 1$ shows a strong peak at 760 cm^{-1} that arises from the merging of two peaks, one at 720 cm^{-1} and another at 770 cm^{-1} , which are seen in glasses with lower x values. Therefore, the peak at 760 cm^{-1} is assigned to the breathing vibrations of ring units containing one or two B^4 units. The weaker bands at 980 and 1102 cm^{-1} arise from vibrations of loose and interconnected diborate groups, respectively.³² The broad peak at 1490 cm^{-1} is assigned to the vibrational modes of the B^2_{B} units. The presence of the B^3 unit can be inferred from the presence of more polymerized, less modified, superstructural units such as the diborate and triborate, $0.25\text{Na}_2\text{O} + 0.75\text{B}_2\text{O}_3$, units, and the limited amount of available sodium, $\text{Na}_2\text{O} = 0.35$, which requires the presence of unmodified SRO structural units, B^3 . We will quantify the composition dependence of all of these units below by using a combination of Raman, ^{31}P , and ^{11}B MAS NMR spectroscopies.

3.2. Intermediate Range Order Structure of the Glasses from Raman Spectroscopy. The decreasing frequencies of the peaks due to P^3 and P^2 units in the Raman spectra with increasing boron contents may also indicate a change in IRO structure of the glasses. For example, in the Raman spectra of ternary glasses, the P^3 peak at 1318 cm^{-1} shifts approximately -115 cm^{-1} to lower frequencies with changing glass composition from $x = 0$ to $x = 0.8$. Likewise, the P^2 peak at 1162 cm^{-1} shifts -63 cm^{-1} to lower frequencies with changing glass composition from $x = 0$ to $x = 0.9$. To determine the origin of these frequency shifts, we must first determine if such frequency shifts occur in the binary glasses that contain P^3 or P^2 units in the $0.35 \leq y \leq 0.66$ range. The work of Nelson et al.³⁴ shows that the wavenumber shifts of the P^3 and P^2 peaks with changing sodium content in binary sodium phosphate glasses are -40 and -23 cm^{-1} , respectively, between 33 and 66% Na_2O . In the binary glasses, these authors attributed these shifts to changing numbers of $P^3\text{--O--P}^2$ and $P^2\text{--O--P}^1$ links caused by the changing sodium content. Since the wavenumber shifts in the spectra of the ternary glasses are much larger than those in the spectra of the binary sodium phosphate glasses, -115 versus -40 cm^{-1} and -63 versus -23 cm^{-1} , respectively,

it is reasonable to assume that there must be additional factors causing the shifts in the peak positions in the Raman spectra of the ternary glasses other than increased modification by sodium. One obvious possibility is to attribute shifts in peak positions to increasing numbers of P–O–B links on the P^3 and P^2 units. We further explore this structural hypothesis below when we examine the ^{31}P and ^{11}B MAS NMR spectra of these glasses.

3.3. ^{31}P MAS NMR Spectra of the Glasses. The central peak and first two satellite transitions of the ^{31}P MAS NMR spectra were fitted with the minimum number of Gaussian curves needed to achieve a good fit with a residual error of less than 3%. An example of the fitting of a typical spectra in this series of glasses is shown in Figure 7. The SRO structural units

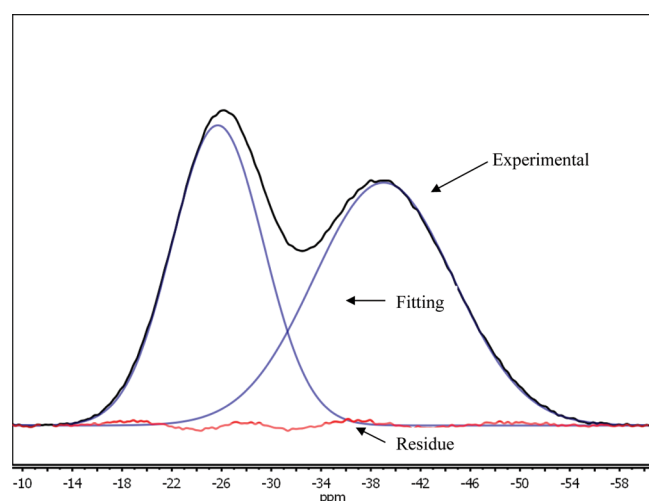


Figure 7. Example of the fitting of the ^{31}P MAS NMR spectra of the $x = 0$ glass.

present at each composition x were identified by use of the SRO structural units present in the binary glasses, $y\text{Na}_2\text{O} + (1 - y)\text{P}_2\text{O}_5$, by use of their chemical shift ranges as established in the literature,³⁵ and by the examination and assignments made in the Raman spectra presented and described above. The compositional dependence of the ^{31}P MAS NMR spectra of all glasses is shown in Figure 8.

3.3.1. ^{31}P MAS NMR Spectra of the $x = 0$ Glass. Literature studies using ^{31}P NMR spectroscopy^{17,19} and Van Wazer's fully ionic model have shown that a binary $0.35\text{Na}_2\text{O} + 0.65\text{P}_2\text{O}_5$ glass is composed of $\sim 54\%$ P^3 and $\sim 46\%$ P^2 SRO structural units.³⁶ As such, the resonances at -26 and -39 ppm in the ^{31}P MAS NMR spectra of the $x = 0$ glass, Figure 8, are assigned to the resonances of the P^2 and P^3 SRO structural units, respectively, and spectral deconvolution and area analysis of the experimental data gives the exact same atomic percentages, 54% P^3 and 46% P^2 , as reported in the literature.

3.3.2. ^{31}P MAS NMR Spectra of the $0.1 \leq x \leq 0.8$ Glasses. As boron is substituted for phosphorus in the network of the ternary glasses, the chemical shift of the P^3 and P^2 peaks increases in frequency with x . This shift in frequency indicates that the phosphorus nucleus is becoming less shielded by the electrons surrounding the nucleus. In the binary sodium phosphate glasses, a shift to higher frequencies (higher ppm values) is associated with the depolymerization of the phosphorus network, $P^3 \rightarrow P^2$, $P^2 \rightarrow P^1$, and $P^1 \rightarrow P^0$. These changes in the SRO must result in changes in the IRO. For

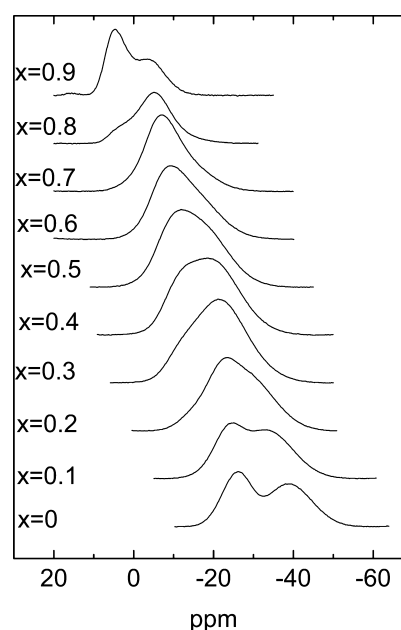


Figure 8. The compositional dependence of the chemical shift of the primary peaks in ^{31}P MAS NMR.

example, with increasing Na content, $P^3_{P3} \rightarrow P^3_{P2}$, $P^2_{P3} \rightarrow P^2_{P2}$, and $P^2_{P2} \rightarrow P^1_{P2}$.¹⁷ Therefore, in order to examine if the chemical shift in the ^{31}P MAS NMR spectra is a result of depolymerization of the phosphorus network or other changes in IRO, such as the substitution of B in the second coordination sphere, we compared the magnitude of the change in the chemical shifts of the ^{31}P MAS NMR resonances in the ternary glasses to the changes in chemical shifts in the binary glasses.

In the $0.35\text{Na}_2\text{O} + 0.65[x\text{B}_2\text{O}_3 + (1 - x)\text{P}_2\text{O}_5]$ ternary glasses, the P^3 peak is first observed in the $x = 0$ glass at -39 ppm and is last observed in the $x = 0.8$ glass at approximately -16 ppm (see Figure 8), a change of $+23$ ppm. P^3 groups are present in binary sodium phosphate glasses, $y\text{Na}_2\text{O} + (1 - y)\text{P}_2\text{O}_5$, over the compositional range of $0 \leq y \leq 0.5$ and changes in the ^{31}P NMR chemical shift of the P^3 groups from -55 to -36 ppm have been observed with changing y ,¹⁷ a change of $+19$ ppm. The chemical shift of the P^3 group in the ternary glasses with changing x is therefore larger than the change in chemical shift seen in the binary glasses, $y\text{Na}_2\text{O} + (1 - y)\text{P}_2\text{O}_5$, over changing y . This suggests that there may be changes in the IRO beyond the increasing fractions of P^3 units bonded to P^2 units. Similar changes must also be occurring in the P^2 structural unit which shifts from -26 to -5 ppm at $x = 0$ to $x = 0.9$, $+21$ ppm, which is larger than the P^2 shift observed in binary $y\text{Na}_2\text{O} + (1 - y)\text{P}_2\text{O}_5$ glasses with changing y , from -32 to -15 ppm, a $+17$ ppm shift overall.

3.3.3. ^{31}P MAS NMR Spectra of the $0.8 \leq x \leq 0.9$ Glasses. At $x = 0.8$, a new peak emerges, which has the chemical shift equivalent to that of a P^1 unit.¹⁹ However, the NMR and Raman literature cited above does not support the existence of P^1 units in binary $y\text{Na}_2\text{O} + (1 - y)\text{P}_2\text{O}_5$ glass until $y \geq 0.5$, well above the nominal glass batched value of 0.35 used here.¹⁹ As we believe this peak to be real and indeed we find spectral evidence for these units in these glasses as described in the Raman spectra of these glasses, this indicates that the ratio of Na bonded to phosphorus, Na:P, is no longer $0.35:65$ as in the binary glass but suggests an Na:P ratio greater than $1:1$, as

would be required to produce the P^1 structural group in the binary glass.

The NMR chemical shifts of the P^1 structural units in the ternary glasses are 3.8–4.8 ppm and lie within the possible chemical shift ranges found for the P^1 group in binary glasses, –8 to 8 ppm. As discussed above, the progressive substitution of B in the second coordination sphere around phosphorus may result in a strong chemical shift effect on the P^1 units, as they can form only one bridge bond to boron. Finally, it is noted that both P_B^3 and P_B^2 units are still present in glasses in the $0.8 \leq x \leq 0.9$ range.

3.4. ^{11}B MAS NMR Spectra. The areas under the curve of the central and first two satellite transitions of the ^{11}B MAS NMR spectra were determined to establish the relative fractions of the boron in trigonal and tetrahedral SRO structural units. The spectral peak arising from the tetrahedral B^4 unit was then fit with the minimum number of Gaussian curves needed to achieve a good fit with a residual error of less than 3%. It was found that, for glasses with $x = 0.1$ and 0.2 , a single B^4 peak was observed, whereas, for glasses with $0.3 \leq x \leq 0.5$, two peaks associated with B^4 units were observed. Finally, for the high borate content and pure borate glasses, $0.6 \leq x \leq 1.0$, again, a single peak for the B^4 units was observed. The SRO structural units present at each composition x were identified by using the SRO structural units present in the binary glasses $y\text{Na}_2\text{O} + (1 - y)\text{B}_2\text{O}_3$ and their chemical shift ranges as established in the literature.^{35,37} The composition dependence of the ^{11}B MAS NMR spectra of the ternary glasses can be seen in Figure 9.

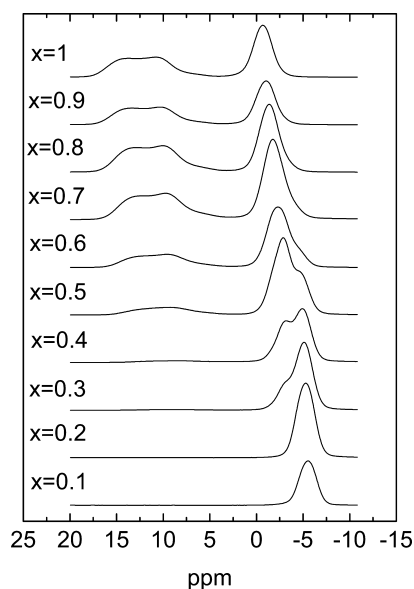


Figure 9. The compositional dependence of the chemical shift of the primary peaks in ^{11}B MAS NMR.

3.4.1. ^{11}B MAS NMR Spectra of the $x = 1$ Glass. As seen in many other studies of binary alkali borate glasses, two primary spectral absorptions were observed in the ^{11}B MAS NMR spectrum of the binary sodium borate glass at $x = 1$, as shown in Figure 9. A quadrupole broadened peak, centered at ~ 12 ppm, arises from the presence of trigonal boron units. A centrally symmetric peak at -0.6 ppm is assigned to the resonance of B_B^4 units where the asymmetry parameter, η , is nearly zero and the quadrupolar broadening effect is removed.

With the addition of phosphorus to the network, these primary peaks shift in the negative ppm, decreasing frequency, direction.

3.4.2. ^{11}B MAS NMR Spectra of the $0.9 \leq x \leq 0.1$ Glasses. At $x = 0.6$, a new B^4 peak appears at -4 ppm, indicating the presence of B^4 units bridging to phosphorus through BOs to form B_P^4 SRO units. For compositions less than $x = 0.3$, the trigonal peak is no longer present, indicating that all boron are in tetrahedral coordination. By $x = 0.2$, the original B^4 peak at -0.6 ppm, B_B^4 , has been completely replaced by the second peak at -5 ppm, indicating that all B^4 units must have at least one BO to phosphorus. The B_B^4 peak replacement by the B_P^4 peak results in a change of chemical shift of -4.9 ppm. Therefore, as the composition changes and the boron content decreases, $x = 1 \rightarrow x = 0.1$, the chemical shift of the B^4 peak moves to lower frequencies.

Van Wullen et al. observed a similar trend in chemical shift in the B^4 peaks of ^{11}B MAS NMR in sodium borosilicate glasses^{38,39} and argued that sodium borosilicate glasses were composed of homogeneously intermixed and interlinked SiO_4 , BO_3 , and BO_4 polyhedra. They found that silicon linked to B^4 groups via BOs increased the shielding of the B^4 unit, thereby reducing the B^4 chemical shift by approximately 0.5 ppm per BO bond. They also found that trigonal boron units linked to B^4 groups via a BO decreased the shielding of the B^4 groups, increasing the chemical shift by approximately 0.5 ppm per BO bond. Likewise, the chemical shift was also found to be more negative if B^4 groups were linked to $\text{SiO}_{4/2}$ or $\text{BO}_{4/2}$ tetrahedra rather than trigonal boron units. Similar work by Elbers et al. was conducted on silver borophosphate glasses in which multiple B^4 signals were observed in the ^{11}B MAS NMR spectra.¹⁵ Further ^{11}B and ^{31}P REDOR experiments on silver borophosphate glasses showed that the additional signals in the MAS NMR spectra came from B^4 units linked to three or less phosphorus atoms. The findings of Van Wullen et al. and Elbers et al. suggest that the negative change in the chemical shift of the B^4 peaks in the present ^{11}B spectra may be caused by the increased BO linkages of various P units to BO_4 tetrahedra with increasing amounts of P in the glasses.

4. DISCUSSION

4.1. The Presence of BPO_4 Units in the Ternary Glasses. Many other investigations of borophosphate glasses have considered the possibility of BPO_4 structural units present in the glasses, having the same structure as in crystalline BPO_4 . A BPO_4 unit consists of a $(B^4)^-$ unit that is not charge compensated by a Na^+ ion, but by a tetrahedral phosphorus unit with four BOs with a positive charge, $(P^4)^+$. Several authors have proposed the existence of BPO_4 units in sodium borophosphate,^{23,40} lithium borophosphate,⁴¹ and zinc borophosphate⁴² glasses, while others such as Elbers et al.¹⁵ and Duce et al. examined silver and sodium borophosphate glasses, respectively,⁴³ and did not find evidence for the formation of BPO_4 units in their glasses. For example, Rinke et al.⁴⁴ showed that the Raman spectra of BPO_4 crystal has a strong peak at $\sim 490\text{ cm}^{-1}$, weaker peaks at 1120 and 240 cm^{-1} , and finally minor peaks at 465 and 1080 cm^{-1} . In our Raman spectra presented and analyzed above, we do not see evidence of BPO_4 units as we do not see evidence of a peak at 240 cm^{-1} . While the peak in the 490 cm^{-1} region could be associated with BPO_4 structural units in the glass, this seems unlikely as the Raman spectral intensity in this region increases with increasing boron content and remains significant even in the $x = 1$ composition where there is no phosphorus available for the formation of the

BPO₄ structural units. The peak at 1120 cm⁻¹ could also be associated with the presence of BPO₄ units, and this peak is present from 0.3 ≤ *x* ≤ 0.9. However, it is a secondary peak of weak intensity and the lack of the primary peak at 490 cm⁻¹ suggests that BPO₄ structural units are not present in these glasses.

Villa et al.⁴⁵ showed that crystalline BPO₄ has a peak in its ³¹P MAS NMR spectra at -30 ppm, when referenced to 85% H₃PO₄. Our ³¹P MAS NMR spectra for the ternary glasses over the compositional range 0.1 ≤ *x* ≤ 0.6, Figure 8, show a broad peak that covers a range of ppm that includes -30 ppm. However, the fitting of the broad peak with a minimum of curves necessary to achieve a good fit, as shown above, does not require a separate peak for the BPO₄ structural unit. Furthermore, when Brow et al.⁴² and Zyer-Dusterer et al.²³ investigated borophosphate glasses with ¹¹B MAS NMR, they did not find a specific chemical shift associated with BPO₄ units. For these reasons, we conclude that there are no BPO₄ units in our glasses, or if there are they are at such a small concentration as to not be observable by either Raman or ¹¹B and ³¹P NMR spectroscopies.

4.2. The Presence of Phase Separation. Evidence of phase separation in these glasses, that would suggest two separate binary networks, was not observed in the composition dependence of the ionic conductivity and *T_g* thermograms or by visual inspection of the glasses. This suggests that these glasses are homogeneous down to the nanometer length scale, although it must be stated that a detailed SEM/TEM study of these glasses has not been conducted to identify whether a shorter range scale phase separation is present. Furthermore, the compositionally systematic wavenumber shifts of the Raman peaks and chemical shifts of the ³¹P and ¹¹B MAS NMR peaks, which have been assigned to the progressive and continuous changes in B–O–P bonding, all strongly suggest that P and B interact and mix on the IRO scale to form a continuously and homogeneously intermixed network.

4.3. SRO Atomic Fraction Model of the Glasses. As we define the MGFE as a nonlinear, nonadditive change in ionic conductivity, it implies that a linear change in the ionic conductivity would be the expected result should there be a simple noninteraction between the borate and phosphate glass networks. Although expecting linear trends might not be the most accurate assumption, it does create a simple and convenient method of tracking the chemical differences of the ternary glasses from those of the known binary end members. Using the idea of constantly modified glass formers, where all ternary glasses have the same B and P modification as in their respective binary end member glass, i.e., the same Na:B and Na:P ratios, we have created a “constant modifier SRO model” which predicts the fraction of the SRO units present in the glass at each composition, Figure 10, by using the following equations,^{31,36} where *x* and *y* are from the chemical formula *y*Na₂O + (1 - *y*)[*x*B₂O₃ + (1 - *x*)P₂O₅] and *f* is the atomic fraction of SRO units. At *x* = 0 and *x* = 1, the equations yield a good match to the experimentally determined SRO structural speciation.

$$f(B^4) = \frac{y*x}{(1-y)} \quad (1)$$

$$f(B^3) = x - f(B^4) \quad (2)$$

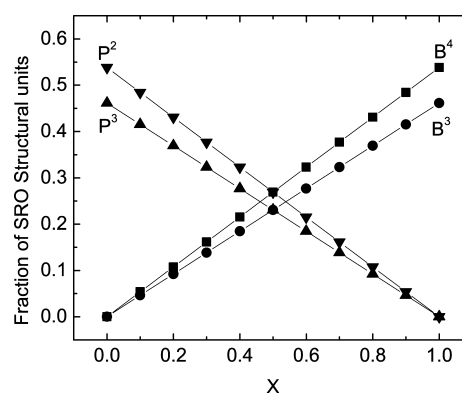


Figure 10. The compositional dependence of the “constant modifier SRO model”.

$$f(P^2) = \frac{y*(1-x)}{(1-y)} \quad (3)$$

$$f(P^3) = (1-x) - f(P^2) \quad (4)$$

We can explore the true, nonlinear nature of the composition, *x*, dependence of the SRO structure of our glasses by using the results of the Raman and NMR spectroscopies in order to create an “atomic fraction SRO model”. In order to quantify the data, the fitted areas of the NMR spectra were scaled by *x* and (1 - *x*) for boron and phosphorus, respectively, to determine their SRO atomic fractions in the ternary glasses. By applying charge neutrality to all compositions, the numbers of Na⁺ ions were required to equal the sum of the numbers of P², 2*P¹, B⁴, and B² groups. Phosphorus and boron structures were confined to the SRO structural units observed in the Raman spectra at each composition, *x*, and the type and fractions of all SRO structural units were adjusted until each sample was charge neutral. These results are shown in Figure 11 and given in Table 1. From the nonlinear trends, it can be immediately seen that the “atomic fraction SRO model” is not in agreement with the “constant modifier SRO model”.

The “atomic fraction SRO model”, Figure 11, shows there are six different SRO structural units present in the 0.35Na₂O + 0.65[*x*B₂O₃ + (1 - *x*)P₂O₅] glasses. At *x* = 0, P³ and P² groups make up 46 and 54% of the SRO structural groups, respectively, in exact agreement with the literature and the Van Wullen

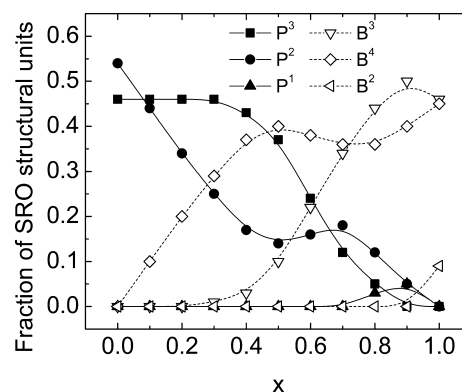


Figure 11. “Atomic fraction SRO model” as determined by Raman and ³¹P and ¹¹B magic angle spinning nuclear magnetic resonance (MAS NMR) spectroscopies.

Table 1. Fraction of Structural Units as Determined by Raman and ^{31}P and ^{11}B Magic Angle Spinning Nuclear Magnetic Resonance (MAS NMR) Spectroscopies

x	P^3	P^2	P^1	B^3	B^4	B^2
0	0.46	0.54	0.00	0.00	0.00	0.00
0.1	0.46	0.44	0.00	0.00	0.10	0.00
0.2	0.46	0.34	0.00	0.00	0.20	0.00
0.3	0.46	0.25	0.00	0.01	0.29	0.00
0.4	0.43	0.17	0.00	0.03	0.37	0.00
0.5	0.37	0.14	0.00	0.10	0.40	0.00
0.6	0.24	0.16	0.00	0.22	0.38	0.00
0.7	0.12	0.18	0.00	0.34	0.36	0.00
0.8	0.05	0.12	0.03	0.44	0.36	0.00
0.9	0.00	0.05	0.05	0.50	0.40	0.00
1	0.00	0.00	0.00	0.46	0.45	0.09

model as discussed above. With the addition of boron, the fraction of P^3 groups remains steady until $x > 0.3$, while the fraction of P^2 groups rapidly decreases as the Na^+ preferentially bonds to the boron to form B^4 units. Although boron is the minority glass former in the $0.1 \leq x \leq 0.3$ region, the preferential bonding of sodium to boron causes the boron to be overly modified, that is, $\text{Na}:\text{B} > 0.35:0.65$, when compared to the $0.35\text{Na}_2\text{O} + 0.65\text{B}_2\text{O}_3$ binary glass, where $\text{Na}:\text{B} = 0.35:0.65$. In the $0.1 \leq x \leq 0.3$ region, the conversion of P^2 units to P^3 units and the simultaneous conversion of the B^3 units to B^4 can be summarized by the chemical reaction, $\text{P}^2 + \text{B}^3 \rightarrow \text{P}^3 + \text{B}^4$.

In the $0.4 \leq x \leq 0.7$ range, boron continues to be overly modified. The fraction of P^2 units passes through a local maximum at $x = 0.7$, while the number of P^3 units decreases in this same composition range. The number of B^4 units reaches a maximum at $x = 0.5$ and the number of B^3 units increases until it reaches a maximum at $x = 0.9$.

In the $0.7 \leq x \leq 0.9$ compositional region, phosphorus is the minority glass former and, as discussed above, is also overly modified compared to the binary $0.35\text{Na}_2\text{O} + 0.65\text{P}_2\text{O}_5$ glasses. This over modification of phosphorus can be seen by the preferential bonding of sodium to phosphorus to form P^1 structural units and by the decrease in the concentration of B^3 units to zero with the addition of P. The behavior continues out to the pure sodium borate, $x = 1$, glass. Hence, a balanced chemical reaction that is consistent with this behavior is $\text{P}^3 + 2\text{B}^2 \rightarrow \text{P}^1 + 2\text{B}^3$. Note that there is the requirement that two B^2 groups react with one P^3 group to produce one P^1 group due to the double negative charge carried by the P^1 group. Whereas, at the other compositional limit, where B is the minority glass former, the slower compositional changes in the fractions of the P^3 and P^2 units with the addition of B arise from the single negative charge on all of the structural SRO units. This behavior explains the rapid decrease in the fraction of the B^2 structural units and the rapid increase in the fraction of the B^3 units in this region, $x = 1 \rightarrow x = 0.8$, yet the slower changes in the fractions of the P^3 and P^2 groups with the addition of B at the other compositional limit, $x = 0 \rightarrow x = 0.3$. However, it remains an open question why the B^4 and P^2 groups are evidently uninvolved in the structural changes taking place in the glasses in this compositional region.

The “atomic fraction SRO model” presented above was found to be in good agreement with the reverse Monte Carlo modeling by Schuch et al.⁴⁶ The work of Schuch et al. was based on the X-ray diffraction study of these glasses by Le Roux et al.⁴⁷ The “atomic fraction SRO model” was also used to

calculate the number of BO and NBOs present in these glasses in a previous work.⁴⁸ The number of BOs present in a glass was compared to the composition dependence of the T_g of the glasses and found to be in excellent agreement. The trend in the number of B^4 units in the “atomic fraction SRO model” with composition was found to have a strong relationship to the number of BOs.

To investigate the underlying cause for the compositional dependence of the various SRO structural groups in these ternary glasses, we provide the start of an answer by examining the Gibbs free energy of formation of the various crystalline compounds corresponding to these SRO groups.

4.4. Solution Thermodynamics of the Ternary Mixed Glass Former System. The results presented above lead to the question, “Why doesn’t the ratio of modifier to glass former remain constant?” To begin to answer this question, we look to the Gibbs free energies of formation of the various SRO structures found in this system and how we can apply our structural model of these glasses to investigate the relative thermodynamic stability of these various structural groups in these glasses. Because these ternary Na B P O compositions appear to form stable and completely reacted homogeneous liquid solutions at the melting temperatures we have used, $\sim 1000^\circ\text{C}$, and appear not to demix or phase separate upon cooling, this suggests that these liquid solutions have achieved a minimum in Gibbs free energy though the various chemical reactions that produce the various SRO structural units that we observe spectroscopically. This suggests a corollary question, “Why is the minimum in free energy of the ternary glasses with variable modification of the structural units more negative than the linear trend in the glass structural groups with constant modification of the glass structure?”

We can begin to answer these questions by using the available data for the Gibbs free energy of formation for each of the SRO units shown in Figures 2 and 3 and calculate the changes in Gibbs free energy as a function of the composition of the liquid (glassy) state SRO structures using both the “constant modifier” and “atomic fraction SRO models”. However, it is recognized that interaction between the borate and phosphate SRO structural units would produce the kinds of mixed IRO structures we have described above and these intermixed bonds would have a contribution to the Gibbs free energies of these glasses. Unfortunately, the thermodynamic values of these mixed structural units are either unknown or poorly known and hence outside of our ability to use them. Nonetheless, it is the formation of the various SRO groups that we are most interested in and it is the thermodynamic properties of the corresponding crystalline compounds that we know the most about, so we begin with the thermodynamic analysis of these structural units.

In these calculations, a few approximations will still have to be made given the lack of complete thermodynamic data that is available for the large numbers of structures and compositions that are reported in this study. We first recognize that the structures are formed at elevated temperatures, $\sim 1000^\circ\text{C}$, and as such we must consider the temperature dependence of the Gibbs free energy as in eq 5, where G is the Gibbs free energy, T is the temperature, and S is the entropy. As we purposefully quenched these liquids from above their corresponding liquidus temperatures into the glassy state in a matter of a few hundred milliseconds, it is reasonable to assume that the SRO structural units that are formed in equilibrium at elevated temperature are nearly those quenched into the room temperature structure of

the glass. The same rapidly increasing viscosity of these liquids with decreasing temperature that allows these liquids to reach the glassy state without crystallizing would also kinetically slow down the chemical reformation with decreasing temperature of the various structural groups in these glasses.

Hence, to be more accurate in these calculations, we must calculate the change in Gibbs free energy of the formation of the various structural units in the liquid state at elevated temperatures. Because of the condensed (solid and liquid) character of these reactions, the entropy change, $\Delta S_{\text{rxn}}(T)$, will be small. Therefore, $\Delta G_{\text{rxn}}(T)$ is likely to have a weak temperature dependence and can be approximated as eq 6.

$$\left(\frac{\partial \Delta G_{\text{rxn}}(T)}{\partial T} \right)_p = -\Delta S_{\text{rxn}}(T) \quad (5)$$

$$\overline{\Delta G_{\text{rxn}}}(T) \sim \overline{\Delta G_{\text{rxn}}}(298 \text{ K}) \quad (6)$$

In order to calculate the Gibbs free energy changes that accompany the formation of the equilibrium compositions for the various SRO structural groups in the series of $0.35\text{Na}_2\text{O} + 0.65[x\text{B}_2\text{O}_3 + (1-x)\text{P}_2\text{O}_5]$ glasses, we used eq 7.

$$\overline{\Delta G_{\text{rxn}}}(T) = \overline{\Delta G_{\text{F}}}(\text{products}, T) - \overline{\Delta G_{\text{F}}}(\text{reactants}, T) \quad (7)$$

$$\overline{\Delta G_{\text{F}}}(\text{reactants}, 298 \text{ K}) = \sum f_i \overline{\Delta G_{\text{F}}}(i)$$

$$\overline{\Delta G_{\text{F}}}(\text{reactants}, 298 \text{ K})$$

$$= f_{\text{Na}_2\text{O}} \overline{\Delta G_{\text{F}}}(\text{Na}_2\text{O}) + f_{\text{B}_2\text{O}_3} \overline{\Delta G_{\text{F}}}(\text{B}_2\text{O}_3) + f_{\text{P}_2\text{O}_5} \overline{\Delta G_{\text{F}}}(\text{P}_2\text{O}_5)$$

where

$$f_{\text{Na}_2\text{O}} = \frac{0.35}{1}$$

$$f_{\text{B}_2\text{O}_3} = \frac{0.65 \cdot x}{1}$$

and

$$f_{\text{P}_2\text{O}_5} = \frac{0.65 \cdot (1-x)}{1}$$

Similarly,

$$\overline{\Delta G_{\text{F}}}(\text{Products}, 298 \text{ K}) = \sum f_i \overline{\Delta G_{\text{F}}}(i)$$

$$\overline{\Delta G_{\text{F}}}(\text{Products}, 298 \text{ K})$$

$$= f_{\text{B}^3} \overline{\Delta G_{\text{F}}}(\text{B}^3) + f_{\text{B}^4} \overline{\Delta G_{\text{F}}}(\text{B}^4) + f_{\text{B}^2} \overline{\Delta G_{\text{F}}}(\text{B}^2) + f_{\text{P}^3} \overline{\Delta G_{\text{F}}}(\text{P}^3) + f_{\text{P}^2} \overline{\Delta G_{\text{F}}}(\text{P}^2) + f_{\text{P}^1} \overline{\Delta G_{\text{F}}}(\text{P}^1)$$

$$\overline{\Delta G_{\text{F}}}(\text{Products}, 298 \text{ K})$$

$$= f_{\text{B}^3} \overline{\Delta G_{\text{F}}}(\text{BO}_{3/2}) + f_{\text{B}^4} \overline{\Delta G_{\text{F}}}(\text{NaBO}_2)_{\text{Tetrahedral}} + f_{\text{B}^2} \overline{\Delta G_{\text{F}}}(\text{NaBO}_2)_{\text{Trigonal}} + f_{\text{P}^3} \overline{\Delta G_{\text{F}}}(\text{PO}_{5/2}) + f_{\text{P}^2} \overline{\Delta G_{\text{F}}}(\text{NaPO}_3) + f_{\text{P}^1} \overline{\Delta G_{\text{F}}}(\text{Na}_2\text{PO}_{7/2})$$

where $\overline{\Delta G_{\text{F}}}(i)$ is the molar Gibbs free energy of formation of the i th structural unit and f_i is the fraction of the i th structural unit in the glass. The Gibbs free energy of formation of

structural units, i , in the crystalline state at 298°C taken from various sources are listed in Table 2. Using these values, the

Table 2. Molar Gibbs Free Energy of Formation of the Various Sodium Borate and Sodium Phosphate SRO Units Found in This System^a

i	$\Delta G_{\text{F}}(i)_{\text{crystal}}$ (kJ/mol)	reference
$\text{BO}_{3/2}$	-597.15	49
NaBO_2 tetrahedral	-950.85	49
NaBO_2 trigonal	-920.70	49
$\text{PO}_{5/2}$	-673.64	50
NaPO_3	-268.32	50
$\text{Na}_2\text{PO}_{7/2}$	-440.27	51
Na_2O	-376.57	49
B_2O_3	-1194.30	49
P_2O_5	-1347.28	50

^aThe value for pure $\text{NaBO}_{4/2}$ structure possessing 100% B^4 units does not exist and was estimated from the values for the $\text{Na}_2\text{B}_4\text{O}_7$ (borax) and B_2O_3 after correcting for the appropriate amounts of B^4 and B^3 groups in each phase.

Gibbs free energy of reaction were calculated using the compositional dependence of the fractions of the SRO structural units of the “constant modifier SRO model” and the “atomic fraction SRO model”.

As can be seen in Figure 12, the Gibbs free energy calculated from the “constant modifier SRO model” and from the “atomic

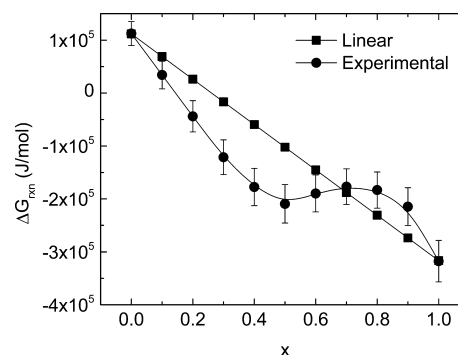


Figure 12. The calculated molar Gibbs free energy of reaction of the “constant modifier SRO model” and the “atomic fraction SRO model” of $0.35\text{Na}_2\text{O} + 0.65[x\text{B}_2\text{O}_3 + (1-x)\text{P}_2\text{O}_5]$ glasses.

fraction SRO model” at $x \geq 0.2$ are both negative and give a thermodynamic basis for why these liquids form stable, homogeneous, fully reacted, and intermixed solutions. The formation of the intermixed SRO structural units of the “atomic fraction SRO model” makes them more thermodynamically stable than glasses of the “constant modifier SRO model” for compositions $0.1 \leq x \leq 0.7$ and suggests why the Na^+ ions are unequally shared between the two glass formers in this range. The main cause of the unequal sharing of the Na^+ ion in this compositional range appears to be associated with the fact that the B^4 unit has the most negative of all the Gibbs free energies of formation of the SRO structural units observed in these glasses. This is at least a partial thermodynamic answer to why the formation of the B^4 group is chemically preferred upon the addition of B_2O_3 to the $x > 0$ compositions. The boron removes the Na^+ from the P^2 units to form more energetically favorable B^4 groups. Even though there are fewer moles of boron than phosphorus in the $0.1 \leq x \leq 0.4$ range, the fact that

the $\overline{\Delta G_F}(B^4)$ is nearly 3.5 times more negative than $\overline{\Delta G_F}(P^2)$ results in an overall decrease in Gibbs free energy.

At this point, it is unknown why the calculated Gibbs free energy of the “atomic fraction SRO model” becomes more positive than that of the “constant modifier SRO model” in the ternary glass compositions at $0.8 \leq x \leq 0.9$, making them appear to be less thermodynamically favorable. Reasons for this thermodynamic favorability of the “constant modifier SRO model” could be due to the inaccuracies of the calculation method. The most obvious of the inaccuracies of the method used is the use of the Gibbs free energy of pure crystalline phases that do not account properly for the effects of neighboring atoms (IRO) in a glass. Other inaccuracies could arise from the treatment of glasses as ideal solutions and the assumption of lack of temperature dependence, among other issues. The effects of IRO in glasses includes the distribution of bond angles and/or bond lengths of the known B–O–B and P–O–P bonds. In addition, the B–O–P bonding we believe to be present in this system must be accounted for as well. We are exploring these inaccuracies in order to improve this modeling.

5. CONCLUSIONS

The SRO and IRO structures of $0.35Na_2O + 0.65[xB_2O_3 + (1-x)P_2O_5]$ glass were examined through Raman and ^{31}P and ^{11}B MAS NMR spectroscopies. Changes in the SRO structures were observed that indicate that the minority glass former has more sodium per glass former than the majority glass former. In the Raman spectra, the IRO of the glasses was also found to change with changing x , although the exact relationship is not known at this time. The changing peak positions of phosphorus in the Raman spectra indicate changes in the next nearest neighbors that cannot be accounted for by changing ratios of P^3 to P^2 links or P^2 to P^1 links caused by changing Na:P ratio. The peak position changes are caused by P–O–B bonding. The MAS NMR spectra showed anomalous chemical shifts in the ternary glasses that could not be accounted for by changing Na:glass-former ratio, also suggesting changing IRO. The large change in the ^{31}P chemical shift of P^3 and P^2 units with increasing x and the decrease in ^{11}B chemical shift of B^4 units with decreasing x indicate that phosphorus is linked to boron through a BO. A thermodynamic treatment was developed that gives some indication of the underlying thermochemical reason for the changing modifier to glass former ratio and strongly suggests that it is the large thermodynamic stability of the B^4 group that drives the unequal sharing of the added modifier in these glasses.

AUTHOR INFORMATION

Corresponding Author

*Phone: (515) 294-045. Fax: (515) 294-5444. E-mail: swmartin@iastate.edu.

Present Address

[†]Department of Chemistry, University of Manitoba, Manitoba, Canada, R3T N2N.

Notes

The authors declare no competing financial interest.

ACKNOWLEDGMENTS

This research was supported by the National Science Foundation under grant number DMR-0710564, and this research support is gratefully acknowledged. The authors would also like to acknowledge the help of NMR spectroscopists Dr.

Shu Xu and Dr. Sarah Cady of the ISU Department of Chemistry, for which we are very grateful.

REFERENCES

- (1) Agarwal, A.; Seth, V. P.; Gahlot, P. S.; Khasa, S.; Arora, M.; Gupta, S. K. Study of Electron Paramagnetic Resonance, Optical Transmission and dc Conductivity of Vanadyl Doped $Bi_2O_3 \cdot B_2O_3 \cdot Li_2O$ Glasses. *J. Alloys Compd.* **2004**, 377 (1–2), 225–231.
- (2) Pradel, A.; Kuwata, N.; Ribes, M. Ion Transport and Structure in Chalcogenide Glasses. *J. Phys.: Condens. Matter* **2003**, 15 (16), S1561–S1571.
- (3) Pradel, A.; Rau, C.; Bittencourt, D.; Armand, P.; Philippot, E.; Ribes, M. Mixed Glass Former Effect in the System $0.3Li_2S \cdot 0.7[(1-x)Si_2-xGeS_2]$: A Structural Explanation. *Chem. Mater.* **1998**, 10 (8), 2162–2166.
- (4) Prasad, P. S. S.; Rani, A. N. D.; Radhakrishna, S. Mixed Glass Former Effect in Silver Iodide-Silver Oxide-Boron Oxide-Arsenic Oxide (mol% 66.67 AgI-24.66 Ag_2O -8.33(1-x) B_2O_3 -x As_2O_3) Quaternary Amorphous Solid Electrolytes. *Solid State Commun.* **1991**, 77 (12), 967–971.
- (5) Prasad, P. S. S.; Rani, A. N. D.; Radhakrishna, S. Mixed Glass Former Effect in Silver Iodide-Silver Oxide-Vanadium Pentoxide Phosphorus Pentoxide Quaternary Amorphous Solid Electrolytes. *Mater. Chem. Phys.* **1990**, 25 (5), 487–499.
- (6) Salodkar, R. V.; Deshpande, V. K.; Singh, K. Enhancement of the Ionic Conductivity of Lithium Borophosphate Glass: A Mixed Glass Former Approach. *J. Power Sources* **1989**, 25 (4), 257–263.
- (7) Jamal, M.; Venugopal, G.; Shareefuddin, M.; Narasimha Chary, M. Sodium Ion Conducting Glasses with Mixed Glass Formers $NaI-Na_2O \cdot V_2O_5 \cdot B_2O_3$: Application to Solid State Battery. *Mater. Lett.* **1999**, 39 (1), 28–32.
- (8) Zielniok, D.; Cramer, C.; Eckert, H. Structure/Property Correlations in Ion-Conducting Mixed-Network Former Glasses: Solid-State NMR Studies of the System $Na_2O \cdot B_2O_3 \cdot P_2O_5$. *Chem. Mater.* **2007**, 19 (13), 3162–3170.
- (9) Kim, Y.; Saienga, J.; Martin Steve, W. Anomalous Ionic Conductivity Increase in $Li_2S + GeS_2 + GeO_2$ Glasses. *J. Phys. Chem. B* **2006**, 110 (33), 16318–16325.
- (10) Christensen, R.; Byer, J.; Olson, G.; Martin, S. W. Ionic Conductivity of Mixed Glass Former $0.35Na_2O + 0.65[xB_2O_3 + (1-x)P_2O_5]$ Glasses. To Be Published, 2011.
- (11) Gedam, R. S.; Deshpande, V. K. An Anomalous Enhancement in the Electrical Conductivity of $Li_2O \cdot B_2O_3 \cdot Al_2O_3$ Glasses. *Solid State Ionics* **2006**, 177 (26–32), 2589–2592.
- (12) Taylor, P. C.; Friebele, E. J. Nature of Unique Boron Sites in Borate Glasses. *J. Non-Cryst. Solids* **1974**, 16 (3), 375–386.
- (13) Prabaker, S.; Rao, K. J.; Rao, C. N. R. ^{11}B NMR Spectra and Structure of Boric Oxide and Alkali Borate Glasses. *Proc. R. Soc. London* **1990**, 429 (1876), 1–15.
- (14) Jellison, G. E.; Bray, P. J. Structural Interpretation of B-10 and B-11 NMR-Spectra in Sodium Borate Glasses. *J. Non-Cryst. Solids* **1978**, 29 (2), 187–206.
- (15) Elbers, S.; Strojek, W.; Koudelka, L.; Eckert, H. Site Connectivities in Silver Borophosphate Glasses: New Results from B-11{P-31} and P-31{B-11} Rotational Echo Double Resonance NMR Spectroscopy. *Solid State Nucl. Magn. Reson.* **2005**, 27 (1–2), 65–76.
- (16) Bray, P. J.; Geissberger, A. E.; Bucholtz, F.; Harris, I. A. Glass Structure. *J. Non-Cryst. Solids* **1982**, 52 (1–3), 45–66.
- (17) Brow, R. K. Review: the Structure of Simple Phosphate Glasses. *J. Non-Cryst. Solids* **2000**, 263 (1–4), 1–28.
- (18) Martin, S. W. Review of the Structures of Phosphate-Glasses. *Eur. J. Solid State Inorg. Chem.* **1991**, 28 (1), 163–205.
- (19) Brow, R. K.; Kirkpatrick, R. J.; Turner, G. L. The Short-Range Structure of Sodium-Phosphate Glasses 0.1. MAS NMR-Studies. *J. Non-Cryst. Solids* **1990**, 116 (1), 39–45.
- (20) Sato, R. K.; Kirkpatrick, R. J.; Brow, R. K. Structure of Li,Na Metaphosphate Glasses by P-31 and Na-23 MAS-NMR Correlated

with the Mixed Alkali Effect. *J. Non-Cryst. Solids* **1992**, *143* (2–3), 257–264.

(21) Villa, M.; Scagliotti, M.; Chiodelli, G. Short Range Order in the Network of the Borophosphate Glasses: A Phosphorus-31 NMR-MAS (Magic Angle Spinning) Study. *J. Non-Cryst. Solids* **1987**, *94* (1), 101–121.

(22) Koudelka, L.; Mosner, P.; Zeyer, M.; Jager, C. Structure and Properties of Mixed Sodium-Lead Borophosphate Glasses. *J. Non-Cryst. Solids* **2005**, *351* (12–13), 1039–1045.

(23) Zeyer-Dusterer, M.; Montagne, L.; Palavit, G.; Jager, C. Combined O-17 NMR and B-11-P-31 Double Resonance NMR Studies of Sodium Borophosphate Glasses. *Solid State Nucl. Magn. Reson.* **2005**, *27* (1–2), 50–64.

(24) Qiu, D.; Guerry, P.; Ahmed, I.; Pickup, D. M.; Carta, D.; Knowles, J. C.; Smith, M. E.; Newport, R. J. A High-Energy X-ray Diffraction, P-31 and B-11 Solid-State NMR Study of the Structure of Aged Sodium Borophosphate Glasses. *Mater. Chem. Phys.* **2008**, *111* (2–3), 455–462.

(25) Bray, P. J.; Okeefe, J. G.; Edwards, J. O.; Tatsuzaki, I.; Ross, V. F. Nuclear Magnetic Resonance Studies of B11 in Crystalline Borates. *J. Chem. Phys.* **1961**, *35* (2), 435.

(26) Meera, B. N.; Ramakrishna, J. Raman Spectral Studies of Borate Glasses. *J. Non-Cryst. Solids* **1993**, *159* (1–2), 1–21.

(27) Kamitsos, E. I.; Chrysikos, G. D. Borate Glass Structure by Raman and Infrared Spectroscopies. *J. Mol. Struct.* **1991**, *247*, 1–16.

(28) Hudgens, J. J.; Brow, R. K.; Tallant, D. R.; Martin, S. W. Raman Spectroscopy Study of the Structure of Lithium and Sodium Ultraphosphate Glasses. *J. Non-Cryst. Solids* **1998**, *223* (1–2), 21–31.

(29) Duce, J. F.; Videau, J. J.; Couzi, M. Structural Study of Borophosphate Glasses by Raman and Infrared-Spectroscopy. *Phys. Chem. Glasses* **1993**, *34* (5), 212–218.

(30) Zhang, Z.; Soga, N. Structural Study of Densified Borate Glasses by Raman and Infrared-Spectroscopy. *Phys. Chem. Glasses* **1991**, *32* (4), 142–148.

(31) Bray, P. J.; O'Keefe, J. G. Nuclear Magnetic Resonance Investigations of the Structure of Alkali Borate Glasses. *Phys. Chem. Glasses* **1963**, *4*, 37–46.

(32) Kamitsos, E. I.; Karakassides, M. A. Structural Studies of Binary and Pseudo Binary Sodium-Borate Glasses of High Sodium Content. *Phys. Chem. Glasses* **1989**, *30* (1), 19–26.

(33) Konijnendijk, W. L.; Stevels, J. M. Structure of Borate Glasses Studied by Raman-Scattering. *J. Non-Cryst. Solids* **1975**, *18* (3), 307–331.

(34) Nelson, C.; Tallant, D. R. Raman Studies of Sodium Phosphates with Low Silica Contents. *Phys. Chem. Glasses* **1985**, *26* (4), 119–122.

(35) Brow, R. K.; Click, C. A.; Alam, T. M. Modifier Coordination and Phosphate Glass Networks. *J. Non-Cryst. Solids* **2000**, *274* (1–3), 9–16.

(36) Van Wazer, J. R. *Phosphorus and its compounds*; Interscience Publishers: New York, 1958.

(37) Michaelis, V. K.; Aguiar, P. M.; Kroeker, S. Probing Alkali Coordination Environments in Alkali Borate Glasses by Multinuclear Magnetic Resonance. *J. Non-Cryst. Solids* **2007**, *353* (26), 2582–2590.

(38) van Wullen, L.; Müller-Warmuth, W. 11B MAS NMR Spectroscopy for Characterizing the Structure of Glasses. *Solid State Nucl. Magn. Reson.* **1993**, *2*, 279–284.

(39) van Wullen, L.; Müller-Warmuth, W.; Papageorgiou, D.; Pentinghaus, H. J. Characterization and Structural Developments of Gel-Derived Borosilicate Glasses: A Multinuclear MAS-NMR Study. *J. Non-Cryst. Solids* **1994**, *171* (1), 53–67.

(40) Anantha, P. S.; Hariharan, K. Structure and Ionic Transport Studies of Sodium Borophosphate Glassy System. *Mater. Chem. Phys.* **2005**, *89* (2–3), 428–437.

(41) Lee, S.; Kim, J.; Shin, D. Modification of Network Structure Induced by Glass Former Composition and Its Correlation to the Conductivity in Lithium Borophosphate Glass for Solid State Electrolyte. *Solid State Ionics* **2007**, *178* (5–6), 375–379.

(42) Brow, R. K. An XPS Study of Oxygen Bonding in Zinc Phosphate and Zinc Borophosphate Glasses. *J. Non-Cryst. Solids* **1996**, *194* (3), 267–273.

(43) Duce, J. F.; Videau, J. J.; Suh, K. S.; Senegas, J. P-31 MAS and B-11 NMR-Study of Sodium Rich Borophosphate Glasses. *Phys. Chem. Glasses* **1994**, *35* (1), 10–16.

(44) Rinke, M. T.; Eckert, H. The Mixed Network Former Effect in Glasses: Solid State NMR and XPS Structural Studies of the Glass System $(\text{Na}_2\text{O})_x(\text{BPO}_4)_{1-x}$. *Phys. Chem. Chem. Phys.* **2011**, *13* (14), 6552–6565.

(45) Villa, M.; Scagliotti, M.; Chiodelli, G. Short-Range Order in the Network of the Borophosphate Glasses - A P-31 NMR-MAS (Magic Angle Spinning) Study. *J. Non-Cryst. Solids* **1987**, *94* (1), 101–121.

(46) Schuch, M.; Christensen, R.; Trott, C.; Maass, P.; Martin, S. W. Investigation of the Structures of Sodium Borophosphate Glasses by Reverse Monte Carlo Modeling to Examine the Origins of the Mixed Glass Former Effect. *J. Phys. Chem. C* **2012**, *116*, 1503–1511.

(47) Le, R. S.; Martin, S.; Christensen, R.; Ren, Y.; Petkov, V. Three-Dimensional Structure of Multicomponent $(\text{Na}_2\text{O})_{0.35}[(\text{P}_2\text{O}_5)_{1-x}(\text{B}_2\text{O}_3)_x]_{0.65}$ Glasses by High-Energy X-ray Diffraction and Constrained Reverse Monte Carlo Simulations. *J. Phys.: Condens. Matter* **2011**, *23*, 035403/1–035403/10.

(48) Christensen, R.; Byer, J.; Olson, G.; Martin, S. W. The Glass Transition Temperature of Mixed Glass Former $0.35\text{Na}_2\text{O}+0.65-[\text{xB}_2\text{O}_3+(1-x)\text{P}_2\text{O}_5]$ Glasses. *J. Non-Cryst. Solids* **2012**, *358* (4), 826–831.

(49) *CRC Handbook of Chemistry and Physics*; CRC Press: Boca Raton, FL; Cleveland, OH, 2011.

(50) Gaskell, D. R. *Introduction to the Thermodynamics of Materials*; Taylor and Francis: Washington, DC, 1995.

(51) Huang, C. T.; Lin, R. Y. Thermodynamics of the Sodium Oxide-Phosphorus Pentoxide System. *Metall. Trans. B* **1989**, *20B*, 197–204.